An Organelle RNA Recognition Motif Protein Is Required for Photosystem II Subunit *psbF* Transcript Editing[1][OPEN]

Justin B. Hackett[2,3], Xiaowen Shi[2,4], Amy T. Kobylarz, Meriah K. Lucas, Ryan L. Wessendorf, Kevin M. Hines, Stephane Bentolila, Maureen R. Hanson, and Yan Lu*

Department of Biological Sciences, Western Michigan University, Kalamazoo, Michigan 49008-5410 (J.B.H., A.T.K., M.K.L., R.L.W., Y.L.); and Department of Molecular Biology and Genetics, Cornell University, Ithaca, New York 14853-2703 (X.S., K.M.H., S.B., M.R.H.)

ORCID IDs: 0000-0001-6532-4522 (J.B.H.); 0000-0001-6532-4522 (X.S.); 0000-0002-6935-9703 (A.T.K.); 0000-0003-2128-5431 (R.L.W.); 0000-0001-6408-5689 (K.M.H.); 0000-0003-2805-7298 (S.B.); 0000-0001-8141-3058 (M.R.H.); 0000-0002-3374-7376 (Y.L.).

Loss-of-function mutations in ORGANELLE RNA RECOGNITION MOTIF PROTEIN6 (ORRM6) result in the near absence of RNA editing of *psbF*-C77 and the reduction in *accD*-C794 editing in Arabidopsis (*Arabidopsis thaliana*). The *orrm6* mutants have decreased levels of photosystem II (PSII) proteins, especially PsbF, lower PSII activity, pale green pigmentation, smaller leaf and plant sizes, and retarded growth. Stable expression of *ORRM6* rescues the *orrm6* editing defects and mutant phenotype. Unlike ORRM1, the other known ORRM plastid editing factor, ORRM6, does not contain RNA editing interacting protein/multiple organellar RNA editing factor (RIP/MORF) boxes, which are required for ORRM1 to interact with site-specific pentatricopeptide repeat protein editing factors. ORRM6 interacts with RIP1/MORF8, RIP2/MORF2, and RIP9/MORF9, known components of RNA editosomes. While some plastid RRM proteins are involved in other forms of RNA processing and translation, the primary function of ORRM6 is evidently to mediate *psbF*-C77 editing, like the essential site-specific pentatricopeptide repeat protein LOW PSII ACCUMULATION66. Stable expression in the *orrm6* mutants of a nucleus-encoded, plastid-targeted PsbF protein from a *psbF* gene carrying a T at nucleotide 77 significantly increases leaf and plant sizes, chlorophyll content, and PSII activity. These transformants demonstrate that plastid RNA editing can be bypassed through the expression of nucleus-encoded, edited forms of plastid genes.

The function of most plant RNA recognition motif (RRM)-containing proteins is unknown. In Arabidopsis (*Arabidopsis thaliana*), 196 genes have been identified that contain sequences encoding RRMs (Lorković and Barta, 2002). Certain plastid RRM proteins are known to be involved in rRNA processing, mRNA splicing, RNA editing, RNA stability, and translation (Yohn et al., 1998; Bonen, 2011; Ruwe et al., 2011; Zoschke et al., 2011; Shi et al., 2016a; Wang et al., 2016).

Recently, Arabidopsis proteins that contain RRM motifs and are organelle targeted have been shown to be required for the efficient editing of different sets of C targets on organelle transcripts. RNA editing in the coding regions of mRNAs restores conserved codons and is thought to be a correction mechanism for defective genes at the transcript level (Lutz and Maliga, 2001; Schmitz-Linneweber and Barkan, 2007; Chateigner-Boutin and Small, 2010, 2011; Dalby and Bonen, 2013; Takenaka et al., 2013; Börner et al., 2014; Sun et al., 2016). Different plant species vary in their numbers of organelle RNA editing sites (Bock, 1998, 2000; Tillich et al., 2005; Li-Pook-Than et al., 2007; Robbins et al., 2009; Wang et al., 2015). To date, 43 plastid and more than 600 mitochondrial C-to-U RNA editing sites have been reported in Arabidopsis (Chateigner-Boutin and Small, 2007; Bentolila et al., 2013; Ruwe et al., 2013).

C-to-U RNA editing is carried out by editosomes, RNA/protein complexes that are between 200 and 400 kD in size (Bentolila et al., 2012; Shi et al., 2016a). Four types of proteins have been identified as C-to-U RNA editing factors in the plastid: PLS subfamily pentatricopeptide repeat (PPR) proteins, RNA editing factor interacting proteins/multiple organellar RNA editing factors (RIPs/MORFs), organelle RNA recognition

[1] This work was supported by the U.S. National Science Foundation (grant nos. MCB-1244008, MCB-1330294, and MCB-1615393) and Western Michigan University (Faculty Research and Creative Activities Award).

[2] These authors contributed equally to the article.

[3] Present address: MD/PhD Program, School of Medicine, Wayne State University, Detroit, MI 48201.

[4] Present address: Division of Biological Sciences, University of Missouri, Columbia, MO 65211.

* Address correspondence to yan.1.lu@wmich.edu.

The author responsible for distribution of materials integral to the findings presented in this article in accordance with the policy described in the Instructions for Authors (www.plantphysiol.org) is: Yan Lu (yan.1.lu@wmich.edu).

J.B.H. and X.S. performed most of the experiments; A.T.K., M.K.L., R.L.W., K.M.H., S.B., and Y.L. carried out some specific experiments; S.B., M.R.H., and Y.L. conceived the project and designed and supervised the experiments; J.B.H., X.S., S.B., M.R.H., and Y.L. analyzed the data and wrote the article.

[OPEN] Articles can be viewed without a subscription.

www.plantphysiol.org/cgi/doi/10.1104/pp.16.01623

 © 2017 American Society of Plant Biologists. All Rights Reserved.

motif-containing proteins (ORRMs), and organelle zinc finger proteins (OZs; Takenaka et al., 2012; Sun et al., 2013, 2015; Barkan and Small, 2014; Colas des Francs-Small and Small, 2014; Shi et al., 2016a). At least one PPR protein, RIP/MORF protein, and ORRM protein are likely to be present in each editosome, which differ in composition in chloroplasts versus mitochondria and between different transcripts in the same organelle (Sun et al., 2016).

PPR proteins involved in editing contain multiple PLS-type PRR repeats, an extension (E) domain, and sometimes a C-terminal DYW domain (O'Toole et al., 2008; Schmitz-Linneweber and Small, 2008; Fujii and Small, 2011; Barkan and Small, 2014) and are site-specific recognition factors for cis-elements near C targets of editing, usually operating on a small number of editing sites (Chaudhuri and Maliga, 1996; Germain et al., 2013; Barkan and Small, 2014; Shikanai, 2015). For example, LOW PSII ACCUMULATION66 (LPA66), a plastid-targeted PPR protein, is specifically required for RNA editing at the *psbF*-C77 site (Cai et al., 2009). C77 is the nucleotide number of the C target relative to the nucleotide A of the translation initiation codon ATG in the *psbF* transcript, which encodes the β-subunit of cytochrome b_{559}.

RIP/MORF proteins contain a conserved RIP/MORF box (Takenaka et al., 2012). One RIP/MORF editing factor (RIP1/MORF8) is dual targeted to plastids and mitochondria, RIP2/MORF2 and RIP9/MORF9 are plastid editing factors, and RIP3/MORF3 and RIP8/MORF1 are required for the editing of many sites in the mitochondrion (Bentolila et al., 2012, 2013; Takenaka et al., 2012). Unlike PPR proteins, RIP/MORF proteins are broadly involved in plastid and/or mitochondrial RNA editing. Fourteen plastid sites and 266 mitochondrial sites are affected in the *rip1/morf8* mutant, and nearly all plastid sites are affected in *rip2/morf2* and *rip9/morf9* mutants (Bentolila et al., 2012; Takenaka et al., 2012). RIP/MORF proteins have been found to interact with PPR proteins via the RIP/MORF box. For example, RIP1/MORF8 interacts with plastid-targeted REQUIRED FOR ACCD RNA EDITING1 (RARE1) and mitochondrion-targeted MITOCHONDRIAL RNA EDITING FACTOR10 (Bentolila et al., 2012; Härtel et al., 2013). RIP/MORF proteins also were found to interact with themselves and other RIP/MORF proteins, suggesting that these proteins may form homo-oligomers and heterooligomers (Takenaka et al., 2012).

Four OZ proteins in Arabidopsis contain multiple Ran-Binding-Protein2 ($CXXCX_{10}CXXC$)-type zinc-finger domains (Sun et al., 2015). A loss-of-function mutation in the *OZ1* gene resulted in a major loss of editing at 14 plastid sites and significant changes in the editing extent at 16 other plastid sites (Sun et al., 2015). Despite the large number of editing sites altered in the *oz1* mutant, C targets on the same transcripts are differentially affected, suggesting that OZ1 action is site specific.

The plastid-targeted ORRM1 was the first member of the ORRM clade among plant RRM proteins to be identified as an editing factor (Sun et al., 2013). Unlike other ORRMs, ORRM1 contains two RIP/MORF boxes, which are required for its interaction with the PPR protein RARE1. The *orrm1* mutant showed nearly complete loss of editing at 12 plastid sites. ORRM2, ORRM3, and ORRM4 are targeted to the mitochondria, and none of them have RIP/MORF boxes. The *orrm2*, *orrm3*, and *orrm4* mutants displayed decreased editing extents at 35, 32, and 262 mitochondrial RNA editing sites, respectively (Shi et al., 2015, 2016b).

In this work, we describe the identification of a unique C-to-U RNA editing factor in the plastid, ORRM6. Unlike the other known ORRM editing factors, loss of ORRM6 primarily affects only two C targets of editing: nearly complete absence of editing at the *psbF*-C77 site and substantial reduction of editing at the *accD*-C794 site, with minor effects on two other sites. We observed that ORRM6 interacts with the plastid RNA editing factors RIP1/MORF8, RIP2/MORF2, RIP9/MORF9, OZ1, and itself, demonstrating that ORRM6 is a component of plastid RNA editosomes. The *orrm6* mutants exhibited reduced photosynthetic efficiency, specifically defective PSII activity. Stable expression of *ORRM6* in the *orrm6* mutants increased the editing extent of *psbF*-C77 and *accD*-C794 and restored most PSII function. Because an RRM protein also could be involved in other types of RNA processing as well as editing, we used a novel assay to determine whether the lack of editing of *psbF* was the primary cause of the mutant phenotype. We introduced a nuclear gene in which C77 had been repaired to a T77 in order to encode the edited form of the protein, which was targeted to the chloroplast by a transit sequence. Stable expression of a nuclear T77 *psbF* gene in the *orrm6* mutants significantly enhanced PSII function and plant growth rate, allowing us to conclude that the *psbF* editing defect was responsible for the mutant phenotype.

RESULTS

Identification of T-DNA Insertion Mutants in a Gene Encoding a Chloroplast-Targeted Protein Carrying an RRM Domain

While examining a collection of mutants in genes encoding proteins carrying putative chloroplast transit sequences (Lu et al., 2008, 2011b; Ajjawi et al., 2011; Yang et al., 2011), we identified two Arabidopsis T-DNA insertion mutants (SAIL_763_A05 and WiscDsLox485-488P23; Fig. 1A) with T-DNA insertions in the first intron of the At1g73530 gene (Fig. 1B), which encodes a 181-amino acid protein (Fig. 1C) with a putative cTP (amino acids 1–44) and an RRM (amino acids 79–148) that is homologous to the RRM of proteins in the ORRM clade of Arabidopsis RRM proteins (Supplemental Fig. S1; Sun et al., 2013). The At1g73530 gene was named *ORRM6* and the two Arabidopsis T-DNA insertion mutants (SAIL_763_A05 and WiscDsLox485-488P23) were named *orrm6-1* and *orrm6-2*, respectively (Fig. 1B). Quantitative reverse transcription (RT)-PCR showed

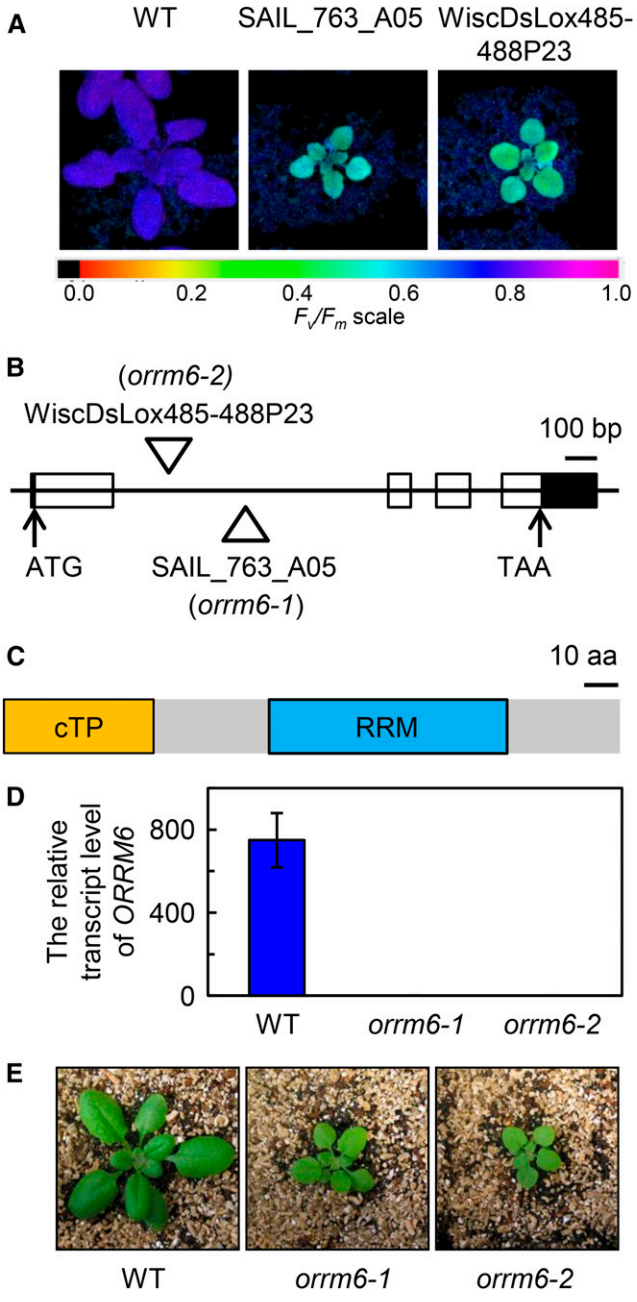

Figure 1. Mutations in the *ORRM6* gene cause reductions in the photosynthetic efficiency of PSII and plant growth. A, False-color images of F_v/F_m. F_v/F_m was measured in 3-week-old plants growing under a 12-h-light/12-h-dark photoperiod. Red pixels indicate that F_v/F_m is below the cutoff value (0.645). WT, Wild type. B, Schematic representation of the *ORRM6* gene and two T-DNA insertion alleles, *orrm6-1* and *orrm6-2*. Black boxes represent untranslated regions (UTRs), and white boxes represent exons. Start and stop codons are indicated as ATG and TAA. T-DNA insertions are shown as white triangles. C, Domains in the full-length ORRM6 protein. The chloroplast transit peptide (cTP; predicted using the TargetP program) is shown as an orange box, and the RRM (predicted by the Pfam program) is shown as a blue box. Bar = 10 amino acids (aa). D, Relative transcript level of *ORRM6*. Total RNA was extracted from mature leaves and analyzed with quantitative RT-PCR. The values (means ± SE, $n = 5$) are presented as ratios to the transcript levels of *ACTIN2* (At3g18780). E, Images of 3-week-old plants. Plants used for chlorophyll fluorescence analysis, quantitative RT-PCR, and photography were grown on a 12-h-light/12-h-dark photoperiod with an irradiance of 150 μmol photons m^{-2} s^{-1} during the light period.

that the presence of the *ORRM6* transcript is completely abolished in *orrm6-1* and *orrm6-2* (Fig. 1D), indicating that these are loss-of-function mutants. Compared with wild-type plants, the *orrm6* mutants are smaller and their leaves are smaller and pale green (Fig. 1E), indicative of growth retardation.

In order to determine the subcellular localization of ORRM6, its full-length coding region was fused with the coding region of a cerulean fluorescent protein (CFP). The transgene was transiently expressed in *Nicotiana benthamiana* leaf cells under the control of the cauliflower mosaic virus (CaMV) 35S promoter (Sparkes et al., 2006; Withers et al., 2012). As shown in Figure 2, the ORRM6-CFP fusion protein colocalizes with chlorophyll autofluorescence, indicating that it is targeted to chloroplasts.

Editing of *accD* and *psbF* Transcripts Is Impaired in the *orrm6* Mutants

The function of only a few of the proteins in the ORRM clade has been identified. ORRM1 is known to be a chloroplast RNA editing trans-factor (Sun et al., 2013), while ORRM2, ORRM3, and ORRM4 are known be required for the editing of mitochondrial RNA editing sites (Shi et al., 2015, 2016b).

Because the RRM of the ORRM6 protein is the most similar to the RRM found in ORRM1 (Fig. 3 in Sun et al., 2013), we performed strand- and transcript-specific PCR sequencing (STS-PCR-seq) to measure RNA editing extents in chloroplast and mitochondrial transcripts. This method combines multiplex RT-PCR amplification of transcripts carrying organellar RNA editing sites with Illumina sequencing, allowing economical and sensitive determination of plastid and mitochondrial RNA editing extents (Bentolila et al., 2013). We analyzed only the *orrm6-2* mutant plants by STS-PCR-seq. Two biological replicates were assayed for each sample, *orrm6-2* mutant plants and wild-type plants. We observed significant decreases only in four plastid RNA editing sites [$P < 1.6e\text{-}6$, Δ (editing) > 0.1; Fig. 3; Supplemental Data Set S1], while none of the mitochondrial sites is affected in the mutant (Supplemental Data Set S1). Two of the affected sites are weakly edited in the wild type and one of the affected sites is in an intron; thus, the small decreases at those two sites in the *orrm6-2* mutant are unlikely to have phenotypic consequences. The two sites that are highly edited in the wild type and significantly decreased in the mutant are *accD*-C794 and *psbF*-C77 (Fig. 3A).

To determine whether these two sites also are affected in *orrm6-1*, we performed Sanger sequencing, which indicates reduced editing at both *accD*-C794

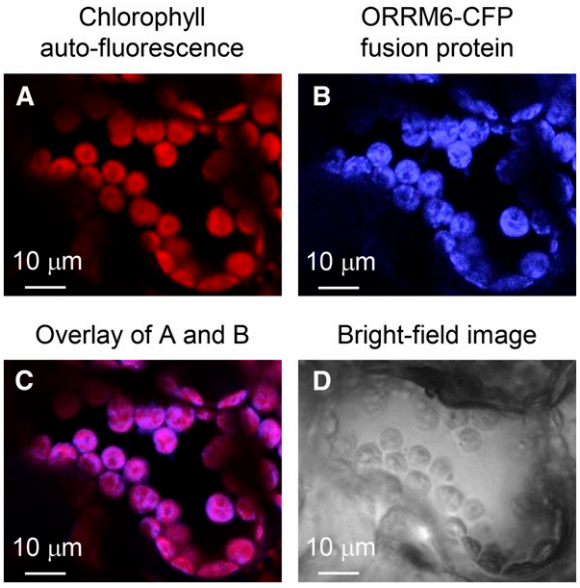

Figure 2. Localization of an ORRM6-CFP fusion protein during transient expression in *N. benthamiana* leaf cells. A, Chlorophyll autofluorescence of *N. benthamiana* mesophyll cells transiently expressing the ORRM6-CFP fusion protein. B, CFP fluorescence of *N. benthamiana* mesophyll cells transiently expressing the ORRM6-CFP fusion protein. C, Overlay of chlorophyll autofluorescence and CFP fluorescence of *N. benthamiana* mesophyll cells transiently expressing the ORRM6-CFP fusion protein. D, Bright-field image of *N. benthamiana* mesophyll cells transiently expressing the ORRM6-CFP fusion protein. Bars = 10 μm.

and *psbF*-C77, with undetectable editing extent in the latter site (Fig. 3B). We confirmed this result by performing poisoned primer extension (PPE), a more sensitive assay for editing extent (Hayes and Hanson, 2007). The PPE assay demonstrates loss of the band corresponding to edited *psbF* transcripts and an increase in the unedited band corresponding to the *accD*-C794 site (Fig. 3C).

Recombinant ORRM6 Protein Binds to the *accD*-C794 and *psbF*-C77 Editing Sites in Vitro

ORRM6 contains an RRM; therefore, we performed RNA electrophoretic mobility-shift assay (REMSA) with affinity-purified 6xHis-tagged ORRM6 protein and fluorescently labeled synthetic *accD*-C794 and *psbF*-C77 as well as *psbE*-C214 RNAs. The synthetic RNAs span 40 nucleotides upstream and 19 nucleotides downstream of the *accD*-C794, *psbF*-C77, and *psbE*-C214 RNA editing sites (Fig. 4). The synthetic *psbE*-C214 RNA was used as a control because *psbE* and *psbF* are on the same polycistronic mRNA. As shown in Figure 4, the proportions of bound RNAs increase as the concentration of 6xHis-tagged ORRM6 increases, and 6xHis-tagged ORRM6 preferentially binds to the *accD*-C794 and *psbF*-C77 RNAs in comparison with the *psbE*-C214 RNA.

Interactions of ORRM6 with Known Editing Factors

We examined pairwise interactions of ORRM6 with other plastid RNA editing factors that are known to be required for efficient editing of either *accD*-C794 or *psbF*-C77. Loss of RIP1/MORF8, RIP9/MORF9, OZ1, and the PPR protein RARE1 in mutants results in reduced or absent editing of *accD*-C794 (Robbins et al., 2009; Sun et al., 2013, 2015). Absence of the PPR protein OZ1 and LPA66 reduces or eliminates the editing of *psbF*-C77 (Cai et al., 2009; Sun et al., 2015). The coding sequences of ORRM1, ORRM6, RIP1/MORF8, RIP2/MORF2, RIP9/MORF9, OZ1, and LPA66 were cloned into XNGW and XCGW Gateway-compatible bimolecular fluorescence complementation (BiFC) vectors, which encode the N- and C-terminal fragments of GFP, respectively (Ohashi-Ito and Bergmann, 2006). Reciprocal BiFC assays showed that ORRM6 interacts with RIP1/MORF8, RIP2/MORF2, RIP9/MORF9, OZ1, and itself when transiently coexpressed in *N. benthamiana* leaves (Fig. 5). No interaction was detected between ORRM6 and the PRR proteins LPA66 and RARE1, or with ORRM1, the other ORRM protein in the plastid (Fig. 5, E–G). In order to verify that LPA66, RARE1, and ORRM1 were expressed properly from the N- and C-terminal BiFC vectors in *N. benthamiana* leaves, we examined their interactions with RIP/MORF and OZ1 proteins. LPA66 interacted with RIP2/MORF2 and RIP9/MORF9, RARE1 interacted with RIP1/MORF8, and ORRM1 interacted with OZ1 (Supplemental Fig. S2).

Photosynthetic Phenotype of the *orrm6* Mutants

In wild-type Arabidopsis, nucleoside C794 is edited to U794 in the *accD* transcript, which introduces a conserved Leu-265 (encoded by UUG; 265 is the amino acid number of the corresponding Leu relative to the first amino acid) instead of Ser-265 (encoded by UCG) in the AccD protein. In wild-type Arabidopsis, editing of C77 in the *psbF* transcript introduces a conserved Phe-26 (encoded by UUU) instead of Ser-26 (encoded by UCU) in the PsbF protein. In the *orrm6* mutants, there are a reduced number of transcripts edited at *accD*-C794 and very few edited *psbF* transcripts, suggesting that PSII function could be affected (Fig. 3; Supplemental Data Set S1).

Because the *orrm6* leaves are pale green, we measured the chlorophyll contents in wild-type and mutant plants grown under standard growth conditions. The content of chlorophyll *a* is 14% and 7% lower in *orrm6-1* and *orrm6-2*, respectively, and the content of chlorophyll *b* is 8% lower in *orrm6-1* and is not reduced significantly in *orrm6-2* (Table I). Consequently, the amount of total chlorophyll is 13% and 6% lower, and the ratio of chlorophyll *a* and *b* is 6% and 4% lower, in *orrm6-1* and *orrm6-2*, respectively.

To further characterize photosynthetic defects in *orrm6-1* and *orrm6-2*, a number of chlorophyll fluorescence parameters were quantified in wild-type and

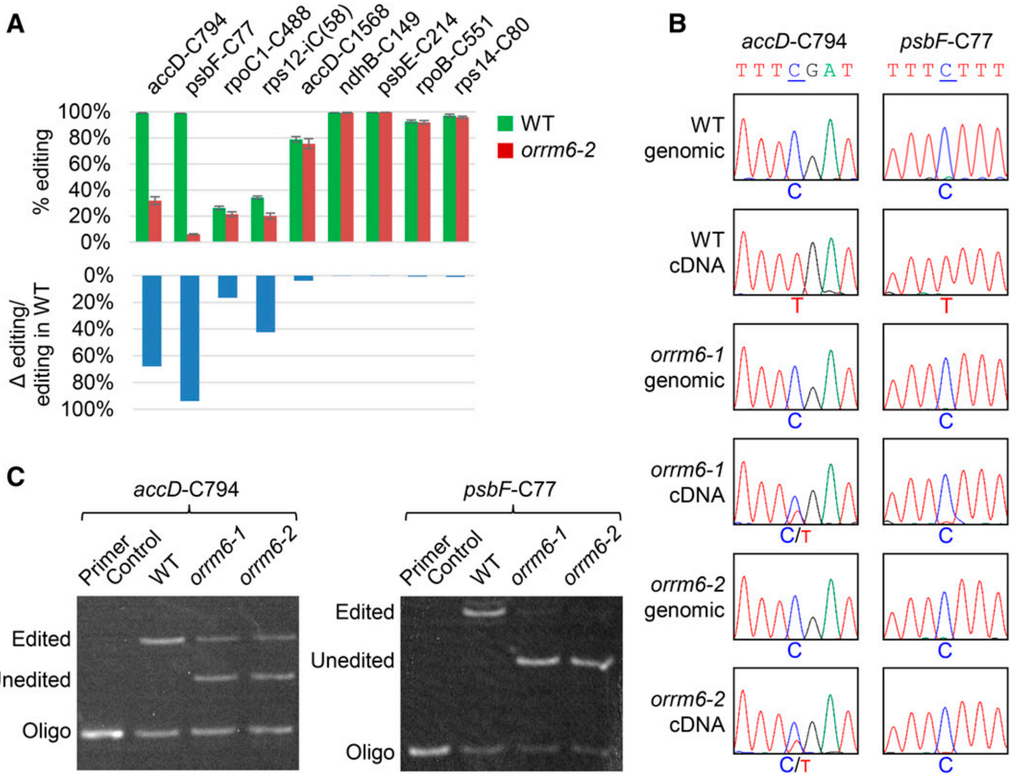

Figure 3. RNA editing at *accD*-C794 and *psbF*-C77 is impaired in the *orrm6* mutants. A, Analysis of RNA editing by STS-PCR-seq. The values (means ± SE) in the top graph are presented as % editing. The values in the bottom graph are presented as (% editing in the wild type [WT] − % editing in *orrm6-2*)/% editing in the wild type. B, Analysis of RNA editing by direct Sanger sequencing. RT-PCR products surrounding *accD*-C794 and *psbF*-C77 were sequenced directly. The seven-nucleotide sequences encompassing *accD*-C794 and *psbF*-C77 are shown. The corresponding genomic sequences of these two sites are displayed as controls. The C nucleotide being edited at the three sites is underlined. C, Analysis of RNA editing by PPE. The fluorescent PPE products of edited and unedited transcripts were separated on denaturing gels (12% polyacrylamide and 7 M urea) and imaged with a fluorescence imager.

mutant plants grown under standard growth conditions. As an indicator of maximum photochemical efficiency of PSII, F_v/F_m is 28% and 35% lower in *orrm6-1* and *orrm6-2*, respectively (Table I), consistent with the initial phenotype of the two mutants (Fig. 1A), indicating that the *orrm6* mutants are unable to utilize the absorbed light energy in photochemistry as efficiently as the wild type. As an indicator of a plant's ability to dissipate excess excitation energy as heat, nonphotochemical quenching (NPQ) is reduced by 51% and 41% in *orrm6-1* and *orrm6-2*, respectively (Table I). NPQ can be split into energy-dependent quenching (qE), state-transition quenching, and photoinhibitory quenching (qI), according to relaxation kinetics (Müller et al., 2001; Baker et al., 2007). Consistent with the reductions in NPQ, qE is reduced by 64% and 51% in *orrm6-1* and *orrm6-2*, respectively (Table I). The NPQ and qE data indicate that the *orrm6* mutants, in comparison with the wild type, dissipate a smaller amount of energy as heat via NPQ. Unlike NPQ or qE, qI in the *orrm6* mutants is not statistically different from that in the wild type (Table I), demonstrating that the *orrm6* mutants experience the same amount of photoinhibition as the wild type under standard growth conditions.

The *orrm6* Mutants Have Reduced Amounts of Nonantenna PSII Proteins

To understand why the *orrm6* mutants have reduced PSII activity, we determined the relative abundances of select PSII proteins in wild-type and mutant plants grown under standard growth conditions. The PSII proteins tested in this study include reaction center core proteins D1 and D2 (i.e. PsbA and PsbD; Psb stands for PSII), core antenna proteins CP43 and CP47 (i.e. PSII chlorophyll proteins of 43 and 47 kD, also known as PsbC and PsbB, respectively), cytochrome b_{559} subunits α and β (i.e. PsbE and PsbF), low-molecular-mass proteins PsbH, PsbI, PsbW, and PsbX, oxygen-evolving complex protein PsbO, PSII light-harvesting chlorophyll *a/b*-binding protein LHCB1, and PsbS, a chlorophyll-binding protein involved in dissipating excess excitation energy via the regulation of NPQ (Lu, 2016). In line with the decreases in F_v/F_m (Table I), the abundances of the 11 nonantenna PSII proteins analyzed in this work, including plastid-encoded PsbA, PsbB, PsbC, PsbD, PsbE, PsbF, PsbH, and PsbI and nucleus-encoded PsbO, PsbW, and PsbX, are reduced significantly in the *orrm6*

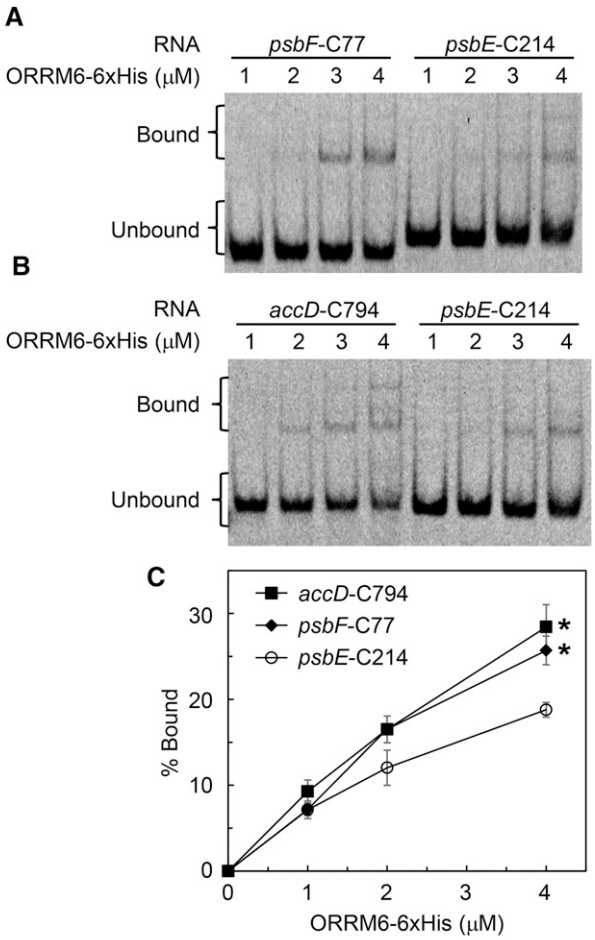

accD-C794 /5ATTO633N/CAUUAUUUGAAAAUGAGUAGUUCAG
AAAGAAUCGAGCUUU**C**GAUUGAUCCGGGUACUUGG
psbF-C77 /5ATTO633N/CGCUGGUUGGCUGUUCAUGGACUAG
CUGUACCUACCGUUU**C**UUUUUUGGGGUCAAUAUCA
psbE-C214 /5ATTO633N/AGCCGACAAGGCAUUCCAUUAAUAA
CAGGCCGUUUUGAUC**C**UUUGGAACAACUCGAUGAA

Figure 4. RNA-binding activity of recombinant ORRM6. A, REMSA gel image with *psbF*-C77 and *psbE*-C214 RNAs. B, REMSA gel image with *accD*-C794 and *psbE*-C214 RNAs. C, Percentages of bound *accD*-C794, *psbF*-C77, and *psbE*-C214 RNAs. REMSA was performed with affinity-purified 6xHis-tagged ORRM6 protein and fluorescently labeled synthetic *accD*-C794, *psbF*-C77, and *psbE*-C214 RNAs (below). The target C in each RNA is boldface and underlined. Asterisks indicate significant differences between the psbE control and the putative target RNAs of ORRM6 (Student's *t* test, *, $P < 0.01$).

mutants (Fig. 6; Supplemental Table S1). The average percentage reduction of the 11 nonantenna PSII proteins in the *orrm6* mutants is 50% (calculated from Supplemental Table S1). Among these proteins, the reduction of the plastid-encoded PsbF protein content in the *orrm6* mutants is most substantial, approximately 80% (Fig. 6; Supplemental Table S1). A PsbF protein with a Ser instead of a Phe at amino acid 26 due to absent editing may be less stable than the wild-type PsbF protein and also may be less functional that the wild-type form. Nevertheless, it is evident that translation of the unedited *psbF* transcripts does occur in the mutants and some protein does accumulate. The PsbS protein level is reduced by 42% in *orrm6-1* and by 30% in *orrm6-2* (Fig. 6; Supplemental Table S1), consistent with the significant decreases of NPQ and qE in the two mutants (Table I). Unlike nonantenna PSII proteins, the LHCB1 protein amount in the *orrm6* mutants is not significantly different from that in the wild type (Fig. 6; Supplemental Table S1).

The Transcript Levels of the Corresponding PSII Genes Are either Unchanged or Increased Significantly in the *orrm6* Mutants

To test whether the reduced amounts of nonantenna PSII proteins in the *orrm6* mutants are due to reduced transcript levels of the corresponding PSII genes, we determined the relative transcript levels of these genes with quantitative RT-PCR. The *psbA* transcript level is 38% and 115% higher in *orrm6-1* and *orrm6-2*, respectively, than in the wild type; the *psbB* transcript level is 106% higher in *orrm6-2* than in the wild type; and the *psbI* transcript level is 83% higher in *orrm6-2* than in the wild type (Supplemental Fig. S3). The transcript levels of the other PSII or PSII-related genes, including plastid-encoded *psbC*, *psbD*, *psbE*, *psbF*, and *psbH* and nucleus-encoded *PsbO1*, *PsbO2*, *PsbS*, *PsbW*, *PsbX*, and *LHCB1* are not significantly different between the wild type and the *orrm6* mutants (Supplemental Fig. S3). Taken together, the transcript levels of the 13 PSII or PSII-related genes analyzed in this study are either unchanged or increased significantly in the *orrm6* mutants, indicating that the reduced amounts of nonantenna PSII proteins in the *orrm6* mutants are not due to reduced transcript levels of the corresponding PSII genes.

Stable Expression of ORRM6 Increases Editing and Restores Photosynthetic Efficiency in the *orrm6* Mutants

We examined whether the stable expression of ORRM6 could complement the T-DNA insertion mutation in this gene. The coding sequence of ORRM6 was cloned into the pPH5ADEST-CFP Gateway binary vector, which is under the control of a CaMV 35S promoter. The pPH5ADEST-ORRM6-CFP construct was introduced into wild-type, *orrm6-1*, and *orrm6-2* mutant plants via an *Agrobacterium tumefaciens*-mediated floral dip method (Clough and Bent, 1998). Hygromycin-resistant plants were selected at the T1 generation, genotyped to verify transformation, and used for SDS-PAGE and immunodetection of the fusion protein with the anti-CFP antibody. Hygromycin-resistant T2 plants of transformants expressing the fusion protein were used for downstream characterization.

The *orrm6-1/ORRM6* and *orrm6-2/ORRM6* plants (i.e. *orrm6-1* and *orrm6-2* mutants expressing ORRM6) are substantially larger than *orrm6* empty-vector control

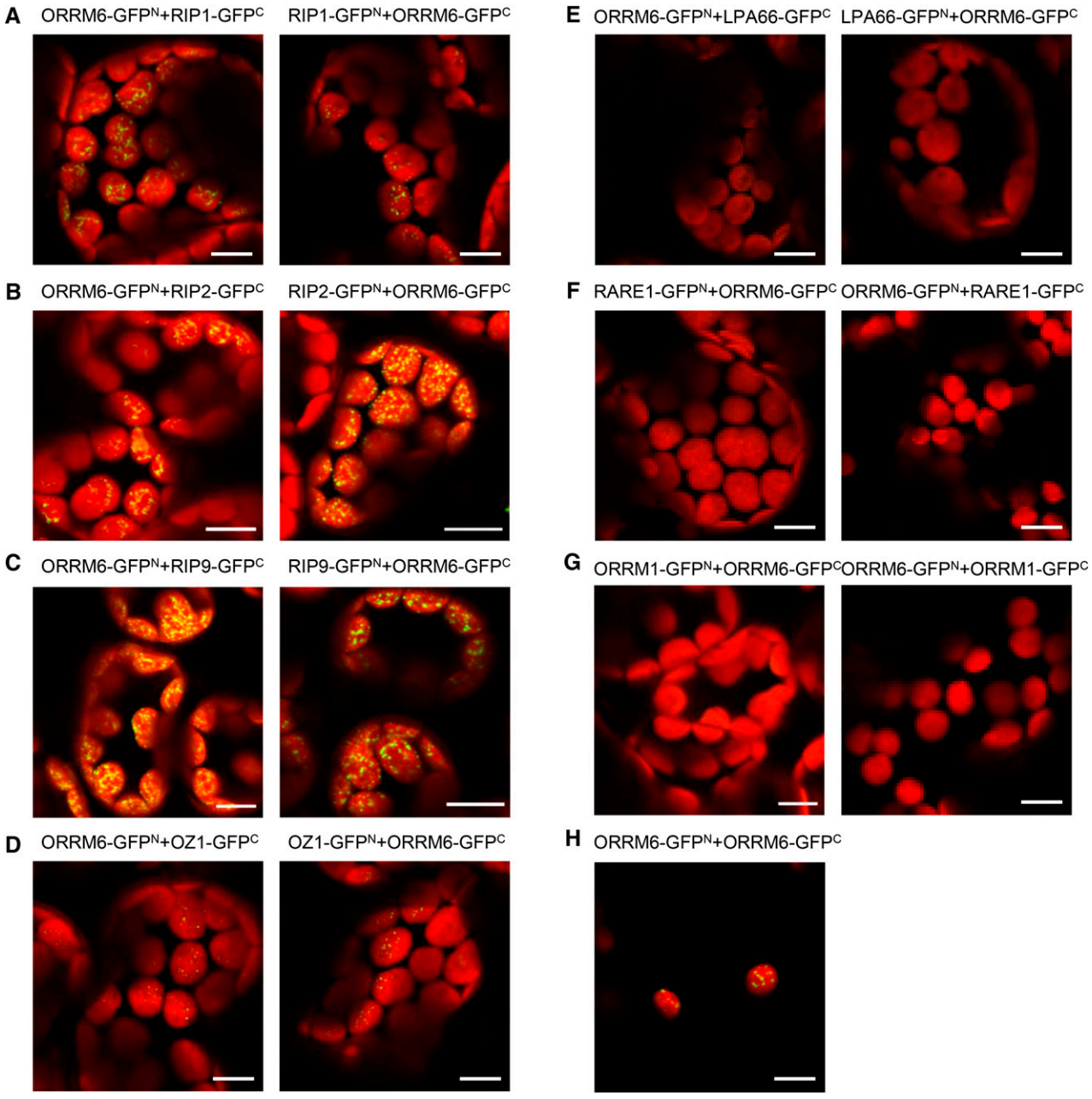

Figure 5. Reciprocal BiFC assays of interactions of ORRM6 and other editing factors fused to either the N-terminal or C-terminal portion of GFP. A to G, Reciprocal BiFC assays between ORRM6 and RIP1/MORF8, RIP2/MORF2, RIP9/MORF9, OZ1, LPA66, RARE1, and ORRM1, respectively. H, BiFC assay of ORRM6 with itself. Each confocal image shows the merge of GFP signal (green) and chlorophyll autofluorescence (red). For simplicity, only one name is shown for proteins with multiple names (e.g. RIP1 for RIP1/MORF8). ORRM6 interacted with RIP1/MORF8, RIP2/MORF2, RIP9/MORF9, OZ1, and itself when transiently coexpressed in *N. benthamiana* leaves but not with ORRM1, LPA66, or RARE1. Positive controls for transient expression of ORRM1, LPA66, and RARE1 in *N. benthamiana* leaves are shown in Supplemental Figure S2. Bars = 10 μm.

plants, nearly indistinguishable in size from wild-type empty-vector control plants (Fig. 7). F_v/F_m of the *orrm6-1/ORRM6* and *orrm6-2/ORRM6* plants is almost at the same level as in wild-type control plants, significantly higher than in *orrm6* empty-vector control mutants (Fig. 7, B and C). The chlorophyll content in the *orrm6-1/ORRM6* and *orrm6-2/ORRM6* plants increases to the wild-type level (Table II). Sanger sequencing of RT-PCR products showed that the editing extents at the *accD*-C794 and *psbF*-C77 RNA editing sites are increased substantially in the *orrm6-1/ORRM6* and *orrm6-2/ORRM6* plants (Fig. 7D).

Table I. *Pigment contents and chlorophyll fluorescence parameters in wild-type and* orrm6 *mutant plants*

Chlorophyll was extracted and determined as described by Wellburn (1994). Measurements of chlorophyll fluorescence parameters were performed with the IMAGING-PAM M-Series chlorophyll fluorescence system (Heinz Waltz) on dark-adapted plants. For NPQ, qE, and qI measurements, an actinic light treatment (531 μmol photons m^{-2} s^{-1}) was performed for 715 s. After termination of actinic light, recovery of F_m' was monitored for 14 min. Data are presented as means ± SE (n = 5 for pigment contents and n = 4 for chlorophyll fluorescence parameters). Asterisks indicate significant differences between the mutant and the wild type (Student's t test: *, $P < 0.05$; **, $P < 0.01$; and ***, $P < 0.001$). Plants used for pigment extraction and chlorophyll fluorescence analysis were grown on a 12-h-light/12-h-dark photoperiod with an irradiance of 150 μmol photons m^{-2} s^{-1} during the light period.

Parameter	Wild Type	*orrm6-1*	*orrm6-2*
Chlorophyll *a* (mg g^{-1} fresh weight)	1.097 ± 0.016	0.944 ± 0.024***	1.022 ± 0.010**
Chlorophyll *b* (mg g^{-1} fresh weight)	0.263 ± 0.004	0.241 ± 0.007*	0.255 ± 0.004
Total chlorophyll (mg g^{-1} fresh weight)	1.360 ± 0.020	1.184 ± 0.031**	1.277 ± 0.014*
Chlorophyll *a*/*b*	4.179 ± 0.031	3.922 ± 0.029***	4.004 ± 0.026**
F_v/F_m	0.827 ± 0.004	0.598 ± 0.013***	0.538 ± 0.003***
NPQ	2.263 ± 0.117	1.099 ± 0.043***	1.325 ± 0.085***
qE	1.861 ± 0.090	0.676 ± 0.055***	0.920 ± 0.092***
qI	0.402 ± 0.029	0.423 ± 0.022	0.405 ± 0.014

Stable Expression of a Nucleus-Encoded, Plastid-Targeted, T-Containing *psbF* Gene Partially Rescues the *orrm6* Mutant Phenotype

Among the RNA editing sites that are affected in the *orrm6* mutants, *psbF*-C77 is most substantially impaired (Fig. 3; Supplemental Data Set S1). Therefore, we tested whether stable expression of nucleus-encoded *psbF* transcripts with a T at position 77 could rescue the *orrm6* mutant phenotype. We designed a plastid-targeted T77 *NEpsbF* (where NE refers to nucleus-encoded) construct that contains the 72-bp 5′ UTR and the 180-bp cTP of the *PsbS* (At1g44575) gene (Kiss et al., 2008; Levey et al., 2014), the coding sequence of T77 *NEpsbF* without the stop codon, the coding sequence for the triple human influenza hemagglutinin (3xHA) tag, and a stop codon (Fig. 8). The 5′ UTR and cTP of PsbS were used to target the transgenic NEPsbF protein into the chloroplast. This construct was custom synthesized and subcloned into the DF264 binary vector, which contains a CaMV 35S promoter and a nopaline synthase polyadenylation signal (Fang and Fernandez, 2002; Lu et al., 2006). The DF264-PsbS(cTP)-T77 NEPsbF-3xHA construct (Fig. 8A) was transformed into wild-type, *orrm6-1*, and *orrm6-2* Arabidopsis plants with the *A. tumefaciens*-mediated floral dip method (Clough and Bent, 1998). Gentamycin-resistant plants were selected at the T1 generation, genotyped to verify transformation, and used for SDS-PAGE and immunodetection of the NEPsbF-3xHA fusion protein with the anti-HA antibody. Gentamycin-resistant T2 plants of transformants expressing the NEPsbF-3xHA fusion protein were used for downstream characterization.

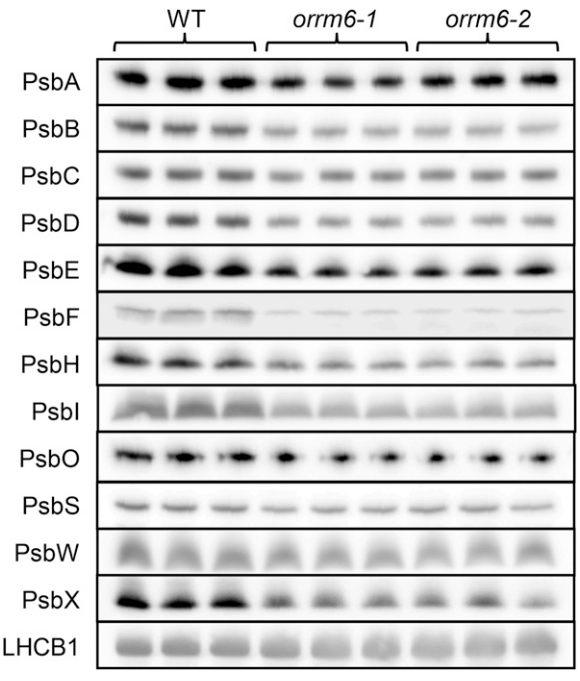

Figure 6. SDS-PAGE and immunoblot analysis of select PSII proteins in wild-type (WT) and *orrm6* mutant plants. Thylakoid membrane proteins were extracted from leaves and loaded on an equal chlorophyll basis. Plants used for SDS-PAGE and immunoblot analysis were grown on a 12-h-light/12-h-dark photoperiod with an irradiance of 150 μmol photons m^{-2} s^{-1} during the light period.

SDS-PAGE and immunoblot analysis confirmed the expression of the NEPsbF-3xHA fusion protein in wild-type and *orrm6* mutant plants transformed with the T77 *NEpsbF* construct (Fig. 8B). The expression of the NEPsbF protein in the *orrm6* mutants resulted in increased levels of other PSII core proteins, such as PsbA, PsbB, and PsbC (Fig. 8B). The *orrm6-1*/*NEpsbF* and *orrm6-2*/*NEpsbF* plants (i.e. *orrm6-1* and *orrm6-2* mutants expressing T77 *NEpsbF*) are larger than the *orrm6* mutant plants but smaller than the wild-type plants (compare Figs. 7A and 8C). F_v/F_m of the *orrm6-1*/*ORRM6* and *orrm6-2*/*ORRM6* plants is significantly higher than that of *orrm6* empty-vector control plants but still lower than that of wild-type

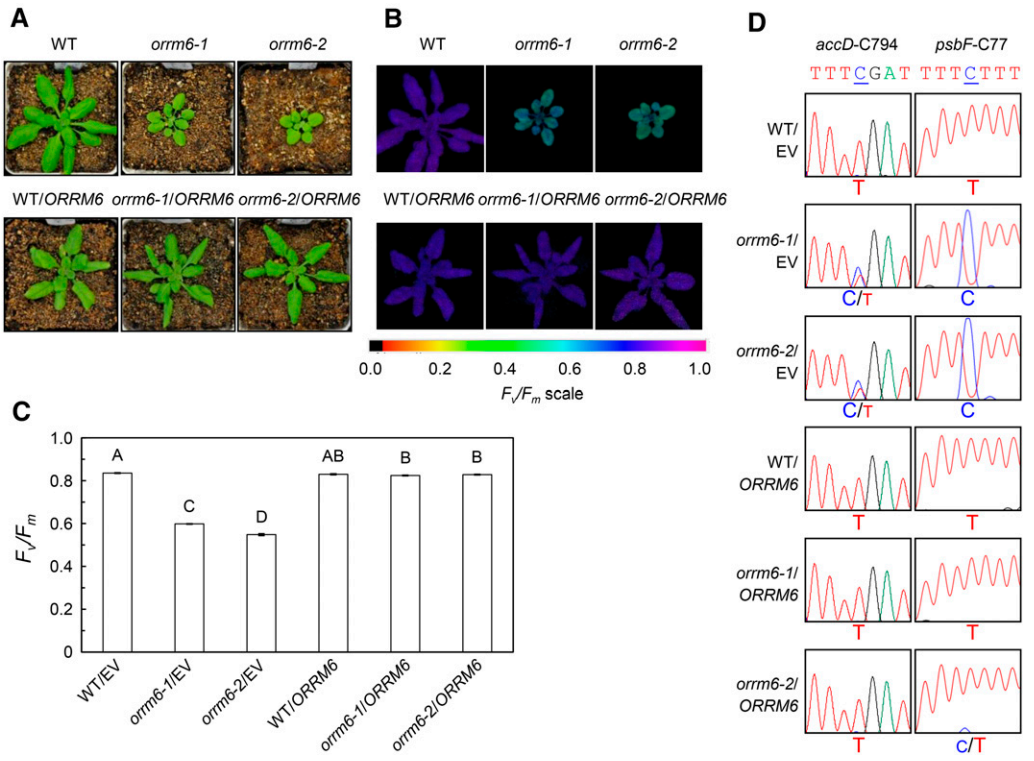

Figure 7. Phenotypes of 4-week-old wild-type (WT) and *orrm6* mutant plants complemented with empty vector or *ORRM6*. A, Images of 4-week-old representative plants. Plants used for pigment contents, chlorophyll fluorescence analysis, and photography were grown on a 12-h-light/12-h-dark photoperiod with an irradiance of 150 μmol photons m^{-2} s^{-1} during the light period. B, False-color F_v/F_m images of 4-week-old representative plants. C, F_v/F_m of 4-week-old representative plants. Data are presented as means ± SE ($n = 14$). Values not connected by the same letter are significantly different (Student's t test, $P < 0.05$). EV, Empty vector. D, Analysis of cDNA sequences at *accD*-C794 and *psbF*-C77. The seven-nucleotide sequences encompassing *accD*-C794 and *psbF*-C77 are shown. The C nucleotide being edited is underlined. Primers accD_1_F and accD_1_R were used to amplify the *accD* transcript and to sequence *accD*-C794. Primers psbF_AtCg00570L and psbF_AtCg00570R were used to amplify the *psbF* transcript, and primer psbF_AtCg00570L was used to sequence *psbF*-C77 RNA.

empty-vector control plants (compare Figs. 7, B and C, and 8, D and E). Bulk sequencing of cDNA from *accD* and *psbF* indicates that unedited *psbF* transcripts can still be detected in the plants containing the nucleus-encoded *psbF* (Fig. 8F). Thus, these plants may contain a mixture of the proper PsbF and PsbF encoded by unedited transcripts, potentially impairing PsbF function. These data demonstrate that stable expression of a nucleus-encoded, plastid-targeted *psbF* gene with the edited nucleotide genomically encoded could partially rescue the photosynthetic phenotype in mutants unable to edit *psbF*-C77 in plastid-encoded transcripts.

DISCUSSION

Loss of Editing at *psbF*-C77 Causes the Observed *orrm6* Mutant Phenotype

Editing assays consistently demonstrate that ORRM6 is required for RNA editing at the *psbF*-C77 and *accD*-C794 sites in the Arabidopsis plastid (Fig. 3; Supplemental Data Set S1). Stable expression of ORRM6 results in a nearly complete complementation of the *orrm6* editing defects and mutant phenotype (Fig. 7; Table II).

The *orrm6* mutants are phenotypically similar to a tobacco (*Nicotiana tabacum*) plastome mutant in which the spinach (*Spinacia oleracea*) *psbF*-C77 editing site was heterologously introduced (Bock et al., 1994; Bock and Koop, 1997; Bondarava et al., 2003). In wild-type tobacco, codon 26 (UUU) encodes Phe and, therefore, does not require C-to-U RNA editing to produce the conserved amino acid in PsbF. In the tobacco plastome mutant with the spinach *psbF*-C77 editing site, codon 26 (UCU) encodes Ser rather than Phe (Bock et al., 1994; Bondarava et al., 2003). However, because tobacco plants do not have one or more proteins required to mediate RNA editing at this heterologous site, the unedited version of PsbF is produced, resulting in pale green leaves, reduced photosynthetic efficiency, and delayed growth and development (Bock et al., 1994; Bondarava et al., 2003). The plastid RNA editing defects in the tobacco plastome mutant could be partially restored transiently by combining the tobacco plastome mutant chloroplast with the nucleocytoplasm from a

Table II. *Pigment contents in wild-type and orrm6 mutant plants complemented with ORRM6 or NEpsbF*

Chlorophyll was extracted and determined as described by Wellburn (1994). Data are presented as means ± SE (n = 4–5 for pigment contents). Values not connected by the same letter are significantly different (Student's t test, $P < 0.05$).

Parameter	Wild Type/Empty Vector	*orrm6-1*/Empty Vector	*orrm6-2*/Empty Vector	Wild Type/*NEpsbF*	*orrm6-1*/*NEpsbF*	*orrm6-2*/*NEpsbF*	Wild Type/*ORRM6*	*orrm6-1*/*ORRM6*	*orrm6-2*/*ORRM6*
Chlorophyll *a* (mg g^{-1} fresh weight)	0.996 ± 0.055^{A}	0.863 ± 0.015^{C}	0.882 ± 0.017^{BC}	1.015 ± 0.025^{A}	0.974 ± 0.035^{AB}	0.954 ± 0.021^{ABC}	1.046 ± 0.050^{A}	1.027 ± 0.045^{A}	1.055 ± 0.023^{A}
Chlorophyll *b* (mg g^{-1} fresh weight)	0.258 ± 0.013^{ABC}	0.239 ± 0.004^{C}	0.256 ± 0.005^{ABC}	0.242 ± 0.007^{BC}	0.268 ± 0.007^{AB}	0.270 ± 0.005^{A}	0.261 ± 0.011^{ABC}	0.251 ± 0.012^{ABC}	0.262 ± 0.006^{ABC}
Total chlorophyll (mg g^{-1} fresh weight)	1.254 ± 0.068^{A}	1.102 ± 0.019^{C}	1.137 ± 0.021^{BC}	1.257 ± 0.031^{A}	1.242 ± 0.041^{A}	1.224 ± 0.025^{ABC}	1.307 ± 0.036^{A}	1.278 ± 0.057^{A}	1.316 ± 0.029^{A}
Chlorophyll *a*/*b*	3.856 ± 0.040^{C}	3.617 ± 0.010^{D}	3.449 ± 0.025^{E}	4.203 ± 0.049^{A}	3.640 ± 0.068^{D}	3.534 ± 0.042^{DE}	4.002 ± 0.050^{B}	4.101 ± 0.039^{AB}	4.033 ± 0.047^{B}

plant species with the RNA editing machinery required for the RNA editing site (Bock and Koop, 1997).

The *orrm6* mutant phenotype also resembles loss-of-function mutants of *LPA66*, which encodes a PPR protein required for RNA editing at the *psbF*-C77 site (Cai et al., 2009). Both *orrm6* and *lpa66* mutants display nearly complete loss of editing at the *psbF*-C77 site, reduced levels of PSII nonantenna proteins, decreased PSII activity, pale green coloration, and retarded growth. The phenotype of *orrm6* and *lpa66* mutants is in direct contrast to loss-of-function mutants of *RARE1*, which encodes a PPR protein required for RNA editing at the *accD*-C794 site (Robbins et al., 2009). The *rare1* mutant shows no editing at *accD*-C794 but is phenotypically indistinguishable from the wild type under laboratory growth conditions (Robbins et al., 2009).

Expressing a nucleus-encoded, plastid-targeted *psbF* gene (*NEpsbF*) encoding the edited form of the PsbF protein partially rescued the *orrm6* mutant phenotype. The nuclear transformants exhibited larger leaf and plant sizes, chlorophyll content, and PSII activity (Fig. 8; Table II). These data indicate that, in the presence of a suitable cTP, the cytosolically synthesized NEPsbF protein could be imported into chloroplasts, assemble into PSII complexes, and thus overcome the RNA editing defect at the *psbF*-C77 site in the *orrm6* mutants. The cTP we used to target the NEPsbF protein into chloroplasts is the cTP of PsbS, an integral thylakoid membrane protein associated with PSII (Kiss et al., 2008; Levey et al., 2014). Expression of nucleus-encoded, edited versions of plastid proteins, therefore, is one way to bypass the requirement for editing of a plastid transcript. Sufficient expression of the wild-type form of PsbF occurred in the nuclear transformants to substantially improve PSII function, but the presence of protein from unedited transcripts may prevent full restoration of the wild-type phenotype.

ORRM6 Is a New and Unusual Component of Particular Arabidopsis Chloroplast Editosomes

Only one other member of the ORRM clade, ORRM1, has been shown previously to be required for the editing of plastid C targets. Unlike ORRM6, ORRM1 has two RIP/MORF boxes in addition to the cTP and the RRM (Sun et al., 2013). The *orrm1* mutant shows nearly complete loss of editing at 12 plastid sites: *accD*-C1568, *matK*-640, *ndhG*-50, *rpoB*-2432, *rps12*-i-58, four sites on *ndhB*, and three sites on *ndhD* (Sun et al., 2013). Each of the mitochondrial editing factors ORRM2, ORRM3, and ORRM4 is required for efficient editing of a large number of mitochondrial C targets (Shi et al., 2016a). In contrast, only two editing targets exhibit substantial decreases in the *orrm6* mutants: nearly complete loss of editing at *psbF*-C77 and substantial reduction of editing at *accD*-C794 (Fig. 3; Supplemental Data Set S1). Unlike the other ORRM editing factors, ORRM6 is similar to PPR proteins in its site specificity. The PPR motifs in PPR proteins have been shown to bind single-stranded

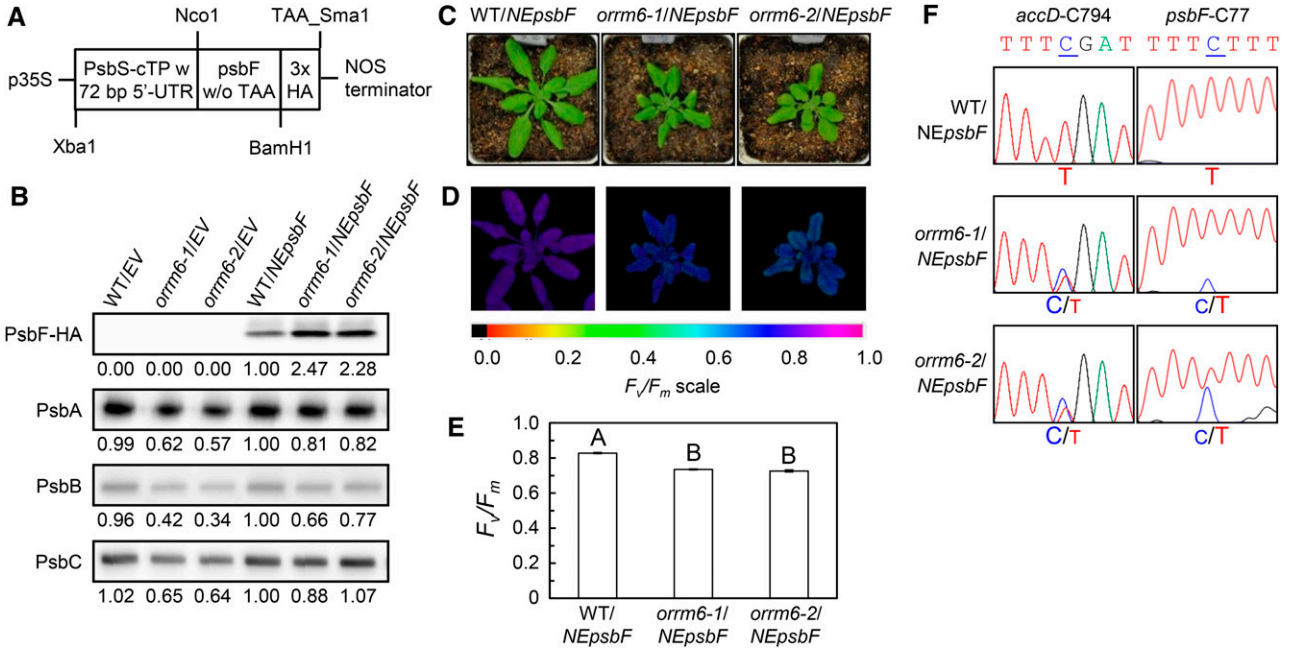

Figure 8. Phenotypes of 4-week-old *orrm6* mutant plants transformed with the T77 *NEpsbF* construct. A, Schematic diagram of the T77 *NEpsbF* construct. The construct contains an *Xba*I restriction digestion site, the 72-bp 5′ UTR, the 180-bp cTP of the *PsbS* (At1g44575) gene, an *Nco*I restriction digestion site, the coding sequence of T77 *NEpsbF* without the stop codon (TAA), a *Bam*HI restriction digestion site, the coding sequence for the triple human influenza hemagglutinin (3xHA) tag, a stop codon (TAA), and the *Sma*I restriction digestion site. This construct is followed by a 260-bp nopaline synthase (NOS) polyadenylation signal. Expression of this fusion gene is under the control of an 800-bp CaMV 35S promoter. B, SDS-PAGE and immunoblot analysis of NEPsbF-3xHA, PsbA, PsbB, and PsbC proteins from 4-week-old representative plants. Total proteins were extracted from leaves, loaded on an equal total protein basis, separated by SDS-PAGE, and detected with the anti-HA antibody. Thylakoid membrane proteins were extracted from leaves, loaded on an equal chlorophyll basis, and detected with the anti-PsbA, anti-PsbB, and anti-PsbC antibodies. Relative abundances of these proteins are indicated below the immunoblot images as ratios to the protein abundances in wild type (WT)/*NEpsbF*. EV, Empty vector. C, Images of 4-week-old representative plants. Plants used for pigment contents, chlorophyll fluorescence analysis, and photography were grown on a 12-h-light/12-h-dark photoperiod with an irradiance of 150 μmol photons m^{-2} s^{-1} during the light period. D, False-color F_v/F_m images of 4-week-old representative plants. E, F_v/F_m of 4-week-old representative plants. Data are presented as means ± SE ($n = 14$). Values not connected by the same letter are significantly different (Student's *t* test, $P < 0.05$). F, Analysis of cDNA sequences at *accD*-C794 and *psbF*-C77. The seven-nucleotide sequences encompassing *accD*-C794 and *psbF*-C77 are shown. The C nucleotide being edited is underlined. Primers accD_1_F and accD_1_R were used to amplify the *accD* transcript and to sequence *accD*-C794. Primers psbF_AtCg00570L and psbF_AtCg00570R were used to amplify the *psbF* transcript, and primer psbF_AtCg00570L was used to sequence *psbF*-C77 RNA.

RNAs in a sequence-dependent manner (Sakamoto et al., 2008; Barkan and Small, 2014). Both ORRM1 and ORRM6 exhibit preferential binding toward RNA editing sites that are affected in loss-of-function mutants (Fig. 4; Sun et al., 2013). PPR and ORRM proteins may both be responsible for recognizing cis-elements near C targets of editing. LPA66 and ORRM6 together may recognize cis-elements near the *psbF*-C77 site, and RARE1 and ORRM6 together may recognize sequences near the *accD*-C794 site. Both ORRM6 and the PPR protein LPA66 have evolved to ensure the editing of *psbF*-C77, indicating the importance of the resultant Phe codon for photosynthetic efficiency and growth.

Interactions of ORRM6 with RIP/MORF editing factors are likely to be essential for the formation of editosomes operating on *psbF* transcripts. ORRM6 interacts with RIP1/MORF8, RIP2/MORF2, and RIP9/MORF9 in BiFC assays (Fig. 5). The lack of interaction of ORRM6 with the PPR protein LPA66, which also is required for *psbF* editing, is not surprising because ORRM6 lacks RIP/MORF domains. ORRM1 interacts with the PPR protein RARE1 via the two RIP/MORF boxes (Sun et al., 2013). RIP/MORF proteins interact with both LPA66 and RARE1. Therefore, it is likely that ORRM6 associates with RIP/MORF proteins, which in turn interact with LPA66 and RARE1 in editosomes operating on *psbF* and *accD* transcripts, respectively. Only weak interaction of ORRM6 with *psbF* RNA could be detected. It is possible that ORRM6 must be complexed with one or more RIP/MORF proteins in order for its RRM domain to be properly configured for RNA-protein interaction. Perhaps ORRM6 enhances binding of the editing complex to the editing site on the *psbF* transcript, working together with the PPR protein LPA66.

ORRM6 interacts with OZ1 (Fig. 5), which is required for many plastid RNA editing sites (Sun et al., 2015). In the loss-of-function *oz1* mutant, 14 plastid RNA editing sites (e.g. *accD*-C794) have major loss of editing, and 16 other plastid sites (e.g. *psbF*-C77) are altered significantly (Sun et al., 2015). Similar to mutants in other editing factors involved in editing at the *psbF*-C77 site, the *oz1* mutant has pale green leaves and retarded growth. Yeast two-hybrid assays showed that OZ1 interacts with ORRM1, RIP1/MORF8, and the PPR proteins CRR28 and OTP82. ORRM6 also was found to interact with itself in BiFC assays (Fig. 5), suggesting that ORRM6 may form oligomers. While the stoichiometry of editing factors present in editosomes is not yet known (Sun et al., 2016), our evidence indicates that the RNA editosomes acting on *psbF*-C77 and *accD*-C794 contain one or more RIP/MORF proteins, OZ1, ORRM6, and either PPR protein LPA66 or RARE1, respectively.

CONCLUSION

Four types of proteins have been found to be required in C-to-U RNA editing in the plastid: PPRs, RIPs/MORFs, ORRMs, and OZs. This work establishes that ORRM6 is necessary for editing *psbF* and *accD* transcripts in the plastid. Loss-of-function mutations in the *ORRM6* gene result in nearly complete loss of editing at *psbF*-C77 and substantial reduction of editing at *accD*-C794. The nearly complete loss of editing at *psbF*-C77 caused significant growth and developmental retardation in the plant. Stable expression of a nucleus-encoded, plastid-targeted T77 *psbF* gene partially rescues the mutant phenotype, demonstrating that plastid RNA editing can be bypassed through the expression of nucleus-encoded, edited forms of plastid genes. ORRM6 interacts with RIP1/MORF8, RIP2/MORF2, and RIP9/MORF9; RIPs/MORFs have been found to interact with PPR proteins. ORRM6 does not interact with the PPR proteins LPA66 and RARE1, which are site-specific recognition factors for the *psbF*-C77 and *accD*-C794 RNA editing sites, respectively. The lack of interaction of ORRM6 with the two PPR proteins is consistent with the absence of the RIP/MORF domain in ORRM6. ORRM1, the other plastid-targeted ORRM protein, interacts with PPR proteins via its two RIP/MORF domains. Taken together, our results suggest that the editosomes operating on *psbF*-C77 and *accD*-C794 contain ORRM6, one or more RIP/MORF proteins, OZ1, and either PPR protein LPA66 or RARE1.

MATERIALS AND METHODS

Plant Materials and Growth Conditions

Arabidopsis (*Arabidopsis thaliana*) T-DNA insertion lines *orrm6-1* (SAIL_763_A05) and *orrm6-2* (WiscDsLox485-488P23) are in the Columbia ecotype and were obtained from the Arabidopsis Biological Resource Center (Sessions et al., 2002; Woody et al., 2007). Homozygosity was confirmed by PCR, using the genotyping primers listed in Supplemental Data Set S2. Plants were grown in a growth chamber on a 12-h-light/12-h-dark photoperiod. The light intensity was 150 μmol photons m^{-2} s^{-1}, the temperature was 22°C, and the relative humidity was 50%. Unless stated otherwise, plants used for pigment measurements, chlorophyll fluorescence, leaf total RNA extraction and subsequent quantitative RT-PCR, Sanger sequencing, as well as thylakoid membrane protein extraction and subsequent immunoblot analysis were 4 weeks old.

Measurement of Chlorophyll Content

Chlorophyll was extracted from rosette leaves with 80% acetone in 2.5 mM HEPES-KOH, pH 7.5, and the amount (mg) of chlorophyll per gram of fresh tissues was measured on a spectrophotometer (Wellburn, 1994).

Chlorophyll Fluorescence Measurements

Chlorophyll fluorescence parameters (F_v/F_m, NPQ, qE, and qI) were measured on dark-adapted plants at room temperature with the MAXI version of the IMAGING-PAM M-Series chlorophyll fluorescence system (Heinz Walz), as described previously (Lu, 2011; Nath et al., 2016, 2017).

Transient Expression of ORRM6-CFP in *Nicotiana benthamiana*

Transient expression of the ORRM6-CFP fusion protein in *N. benthamiana* was performed as described previously (Sparkes et al., 2006; Withers et al., 2012). The full-length *ORRM6* coding region without the stop codon (*ORRM6*$^{1\text{-}547\ bp}$, corresponding to ORRM6$^{1\text{-}181\ aa}$) was amplified using the mRNA:cDNA hybrid, Phusion High-Fidelity DNA Polymerase (New England Biolabs), forward primer ORRM6_F, and reverse primer ORRM6_R (Supplemental Data Set S2). The resulting PCR products were Gateway cloned into the pENTR/D-TOPO vector (Thermo Fisher; Karamoko et al., 2011) and sequenced to confirm the absence of PCR errors. The confirmed *ORRM6*$^{1\text{-}547\ bp}$ fragment was subcloned into the pPH5ADEST-CFP vector (provided by Jian Yao, Department of Biological Sciences, Western Michigan University) using the Gateway LR Clonase II enzyme mix (Thermo Fisher). The resulting pPH5ADEST-ORRM6-CFP construct, which is under the control of a CaMV 35S RNA promoter, was introduced into *Agrobacterium tumefaciens* strain C58C1. Transformed *A. tumefaciens* was cultured overnight at 30°C in Luria-Bertani medium containing appropriate antibiotics, harvested by centrifugation at 3,500 rpm at room temperature for 10 min, washed once in infiltration buffer (10 mM MES, pH 5.8, 10 mM $MgCl_2$, and 0.2% Suc), and resuspended to OD_{600} = 0.2 in infiltration buffer containing 300 μM acetosyringone. The *A. tumefaciens* cultures were syringe inoculated into mature leaves of *N. benthamiana*, and transient expression of the ORRM6-CFP fusion protein was analyzed by confocal microscopy at 36 to 48 h after inoculation.

Extraction of Leaf Total Proteins

Leaf samples were harvested, frozen in liquid nitrogen, and ground into fine power with stainless steel beads and TissueLyser II (Qiagen). Freshly made plant protein extraction buffer (50 mM Tris-HCl, pH 7.5, 150 mM NaCl, 1% Triton X-100, 0.5% sodium deoxycholate, 0.1% SDS, 1 mM EDTA, 1 mM DTT, and 1% plant protease inhibitor cocktail) was added to the frozen power (5 μL mg^{-1} tissues), and the sample was further homogenized with TissueLyser II. The resulting homogenate was centrifuged at more than 10,000*g* for 3 min at 4°C. The supernatant was transferred to a new microfuge tube and centrifuged again at more than 10,000*g* for 3 min at 4°C to remove residual tissue debris. The protein concentration was determined using the DC (for detergent-compatible) protein assay (Bio-Rad) with 0 to 1.4 mg mL^{-1} bovine serum albumin as a standard.

Isolation of Thylakoid Membranes

Thylakoid membranes were isolated as described previously (Lu, 2011; Nath et al., 2016) with minor modifications. The entire aerial portion of plants (~2 g) was excised and ground into fine power in liquid nitrogen with a mortar and pestle. Freshly made grinding buffer (50 mM HEPES-KOH, pH 7.5, containing 330 mM sorbitol, 2 mM EDTA, 1 mM $MgCl_2$, 5 mM ascorbate, 0.05% bovine serum albumin, 10 mM NaF, and 0.25 mg mL^{-1} Pefabloc SC protease inhibitor) was

added to the frozen powder (~10 mL g^{-1} tissues), and the sample was further homogenized by repeated swirling of the pestle. The resulting homogenate was filtered through a layer of Miracloth (EMD Millipore) and centrifuged at 2,500*g* for 4 min at 4°C using a swing-bucket rotor. The pellet was resuspended and centrifuged in resuspension buffer I (50 mM HEPES-KOH, pH 7.5, containing 5 mM sorbitol, 10 mM NaF, and 0.25 mg mL^{-1} Pefabloc SC). The resulting thylakoid pellet was resuspended and centrifuged in resuspension buffer II (50 mM HEPES-KOH, pH 7.5, containing 100 mM sorbitol, 10 mM $MgCl_2$, 10 mM NaF, and 0.25 mg mL^{-1} Pefabloc SC). The final pellet was resuspended in a small volume of resuspension buffer II (~1 mL per 2 g of starting tissues). The chlorophyll in 20 μL of resuspended thylakoid membranes was extracted with 0.98 mL of 80% acetone in 2.5 mM HEPES-KOH, pH 7.5, and the amount of chlorophyll was determined on a spectrophotometer (Wellburn, 1994). The remaining suspension was frozen in liquid nitrogen and stored at −80°C for further use.

SDS-PAGE and Immunoblot Analysis

SDS-PAGE and immunoblot analysis of thylakoid membrane proteins were carried out as described previously (Lu et al., 2011a; Nath et al., 2016) with minor modifications. Proteins loaded on an equal fresh tissue weight basis were separated by SDS-PAGE (15% polyacrylamide and 6 M urea) using a Mini PROTEAN Tetra Cell vertical gel electrophoresis system (Bio-Rad). After electrophoresis, the proteins were transferred to a polyvinylidene difluoride membrane (EMD Millipore) using the Trans-Blot electrophoresis transfer cell (Bio-Rad). The membrane was incubated in the blocking solution (5% nonfat dry milk and 0.1% Tween 20 in 1× Tris-buffered saline) and then in a diluted primary antibody solution. Except for the anti-NFU3 antibody, which was custom made, all other antibodies were purchased from Agrisera. Immunodetection of proteins on the polyvinylidene difluoride membrane was performed using the SuperSignal West Pico rabbit IgG detecting kit (Thermo Fisher) and analyzed with the Gel Logic 1500 Imaging System (Kodak).

Quantitative RT-PCR

Quantitative RT-PCR was performed as described previously (Clark and Lu, 2015). Total RNA was extracted from Arabidopsis rosette leaves using the RNeasy Plant Mini Kit (Qiagen), digested with RNase-Free DNase I (Qiagen), and reverse transcribed with random primers (Promega) and Moloney murine leukemia virus reverse transcriptase (Promega) to generate the mRNA:cDNA hybrids. Quantitative PCR was performed on the StepOnePlus Real-Time PCR System (Thermo Fisher) with the Power SYBR Green PCR master mix (Thermo Fisher) and the quantitative RT-PCR primers listed in Supplemental Data Set S2.

Analysis of Plastid RNA Editing by Sanger Sequencing

The transcript regions encompassing the Arabidopsis plastid RNA editing sites were amplified using Phusion High-Fidelity DNA Polymerase (New England Biolabs) using the PCR amplification/Sanger sequencing primers listed in Supplemental Data Set S2. The resulting PCR products were sequenced directly at the Michigan State University Genomics Facility using the Sanger method and the PCR amplification/Sanger sequencing primers listed in Supplemental Data Set S2. To confirm the defects in RNA editing at *accD*-C794 and *psbF*-C77, genomic DNAs were extracted from wild-type and *orrm6* mutant leaves, and the genomic sequences surrounding the *accD*-C794 and *psbF*-C77 editing sites were amplified and sequenced with appropriate primers.

Analysis of Editing Extents by PPE

RNA editing at the *accD*-C794 and *psbF*-C77 editing sites was analyzed with fluorescent PPE assays, using Pfu DNA polymerase (Stratagene), dATP, dCTP, acyclo-GTP (New England Biolabs), dTTP, fluorescently labeled primers (Integrated DNA Technologies), and cDNAs from the wild type and the *orrm6* mutants, as described previously (Roberson and Rosenthal, 2006). The PPE_accD_1_R and PPE_psbF_1_R primers (Supplemental Data Set S2) were synthesized, labeled with the fluorescent dye ATTO 633 at the 5′ end, purified with the ion-exchange HPLC method, and used in the PPE assay of the *accD*-C794 and *psbF*-C77 editing sites, respectively. The fluorescent PPE products of edited and unedited transcripts were separated on denaturing gels (12% polyacrylamide and 7 M urea) with the model S2 Sequencing Gel Electrophoresis Apparatus (Apogee Electrophoresis) and imaged on the Storm 860 Molecular Imager (Molecular Dynamics).

Analysis of RNA Editing by STS-PCR-Seq

Leaf tissues from 5-week-old wild-type and *orrm6-2* plants were used for STS-PCR-seq analysis of organelle (plastid and mitochondrion) RNA editing extents as described previously (Bentolila et al., 2013). Total leaf RNAs were extracted and reverse transcribed with reverse primer mixes specific for plastid and mitochondrial RNA editing sites (Supplemental Data Set S2). The RT products were subsequently amplified via multiplex PCR, purified, quantified, mixed in equimolar ratio, sheared by sonication, and used for the preparation of TruSeq DNA PCR-Free libraries (Illumina). Analysis of STS-PCR-seq data was performed as described by Bentolila et al. (2013). The statistical analysis to determine which editing site is significantly affected in the *orrm6-2* mutant compared with the wild type is very similar to the one performed previously (Shi et al., 2015, 2016b). Briefly, we performed a χ^2 test with 1 degree of freedom for each mutant biological replicate and each wild-type replicate to test for a significant difference in editing extent. Because of repetitive testing, we chose a nominal error rate of $P < 1.6e\text{-}6$ to achieve the desired family error rate of $P < 1e\text{-}3$ when analyzing 612 sites (36 plastid sites + 576 mitochondrial sites). For a site to be declared significantly affected in the *orrm6-2* mutant, the first condition had to be $P < 1.6e\text{-}6$ for the four χ^2 tests between each biological replicate (*orrm6-2*-1 versus WT-1, *orrm6-2*-1 versus WT-2, *orrm6-2*-2 versus WT-1, and *orrm6-2*-2 versus WT-2). In addition to this χ^2 test requirement, a site was declared significantly reduced in its editing extent in the *orrm6-2* mutant if the reduction compared with the wild-type plant was greater than 0.1 for each biological replicate. The reduction in editing extent is calculated as Δ (editing): (% editing in the wild type − % editing in *orrm6-2*)/% editing in the wild type.

Expression and Purification of the Recombinant ORRM6 Protein in *Escherichia coli*

Expression and purification of the recombinant ORRM6 protein in *E. coli* were performed as described by Lu et al. (2006) with minor modifications. Total Arabidopsis leaf RNA was extracted, digested with RNase-free DNase I, and reverse transcribed with oligo$(dT)_{15}$ primers and Moloney murine leukemia virus reverse transcriptase. The full-length *ORRM6* coding region (*ORRM6*$^{1\text{-}550\ bp}$, corresponding to ORRM6$^{1\text{-}181\ aa}$) and the *ORRM6* coding region lacking the transit peptide (*ORRM6*$^{133\text{-}550\ bp}$, corresponding to ORRM6$^{45\text{-}181\ aa}$) were amplified using the mRNA:cDNA hybrid, Phusion High-Fidelity DNA Polymerase (New England Biolabs), forward primers ORRM6_*Bam*H1_ATG and ORRM6_*Bam*H1_noTP, and reverse primer ORRM6_Xho1_TAG (Supplemental Data Set S2). The resulting PCR products were AT cloned into the pGEM-T Easy Vector (Promega) and sequenced to confirm the absence of PCR errors. *Bam*HI/XhoI-digested *ORRM6* fragments were subcloned into the pET28a expression vector (Novagen) and expressed in *E. coli* strain Rosetta 2 (DE3) (Novagen). An overnight culture of Rosetta 2 (DE3) harboring the *ORRM6*$^{133\text{-}550\ bp}$ gene was diluted 1:20 and grown at 37°C for 1 h. Expression of the recombinant ORRM6$^{45\text{-}181\ aa}$ protein was induced with 1 mM isopropyl β-D-thiogalactoside, and cells were grown at 28°C overnight. The recombinant protein was affinity purified with nickel-nitrilotriacetic acid agarose under native conditions according to the QIAexpressionist protocol (Qiagen).

REMSA

REMSA was performed as described previously (Schallenberg-Rüdinger et al., 2013) with notable exceptions. The 60-nucleotide RNA probes (Fig. 4) were synthesized, labeled with the fluorescent dye ATTO 633 at the 5′ end, purified with ion-exchange HPLC, and diluted to working concentrations in 10 mM Tris-HCl, pH 7.5, and 1 mM EDTA. The RNA probes were incubated at 94°C for 2 min and then on ice for 4 min in 1× REMSA buffer (20 mM NaCl, 2.5 mM Tris-HCl, pH 8, 2 mM DTT 0.01 mg mL^{-1} BSA, 0.05 mg mL^{-1} heparin, and 5% glycerol) to remove secondary structures. Following incubation on ice, 30 units per reaction of SUPERase•In RNase Inhibitor (Thermo Fisher) and an appropriate volume of recombinant ORRM6 protein were added to a total reaction volume of 30 μL. The resulting binding reaction was incubated in the dark at 4°C for 20 min. To separate bound and unbound RNAs, 5% native polyacrylamide gels in 0.5× TBE buffer (44.5 mM Tris-HCl, 44.5 mM boric acid, and 1 mM EDTA) were preelectrophoresed in 0.5× TBE buffer for 30 min at 100 V. After preincubation, 25 μL of samples was loaded and eletrophoresed at

100 V for 1 h. The polyacrylamide gel was imaged on a Storm 860 phosphorimager with a 650-nm excitation and 635-nm emission profile and a 1,000-V photomultiplier. Five to six independent REMSA experiments per RNA sample (*accD*-C794, *psbF*-C77, or *psbE*-C214) were performed. Band intensities were quantified using MultiGauge software (Fujifilm). Using the modified Thompson τ test, one outlier each was identified from the *psbF*-C77 and *psbE*-C214 data. After removal of the two outliers, Student's *t* test was performed to compare the average values between the likely RNA targets of ORRM6 and a control RNA to which ORRM6 would not be expected to bind.

Stable Expression of ORRM6-CFP in Arabidopsis

A. tumefaciens containing the pPH5ADEST-ORRM6-CFP construct was used to transform wild-type, *orrm6-1*, and *orrm6-2* Arabidopsis plants with the floral dip method (Clough and Bent, 1998).

Stable Expression of a Nucleus-Encoded, Plastid-Targeted *psbF* Gene in Arabidopsis

The T77 *NEpsbF* construct shown in Figure 8A was synthesized by Genscript to carry a T at position 77, subcloned into binary vector DF264, and sequenced to confirm the absence of errors. DF264 contains the 800-bp CaMV 35S promoter and the 260-bp nopaline synthase polyadenylation signal (Hajdukiewicz et al., 1994; Fang and Fernandez, 2002; Lu et al., 2006). The binary vector containing the T77 *NEpsbF* construct was transformed into wild-type, *orrm6-1*, and *orrm6-2* Arabidopsis plants with the *A. tumefaciens*-mediated floral dip method (Clough and Bent, 1998).

BiFC Assay

The coding sequences of *ORRM6*, *RIP1/MORF8* (At3g15000), *RIP2/MORF2* (At2g33420), *RIP9/MORF9* (At1g11430), *OZ1* (At5g17790), *LPA66* (At5g48910), *RARE1* (At5g13270), and *ORRM1* (At3g20930) without the stop codon were amplified from full-length cDNAs as described above and in previous studies (Bentolila et al., 2012; Sun et al., 2013, 2015; Shi et al., 2015, 2016b), cloned into the pCR8/GW/TOPO TA vector (Thermo Fisher), and sequenced to confirm the absence of errors. The confirmed fragments were then subcloned into XNGW and XCGW vectors (Ohashi-Ito and Bergmann, 2006) by LR recombination reactions. The two vectors have been used previously to demonstrate interactions between different RNA editing factors, such as ORRM4 and RIP1/MORF8 (Shi et al., 2016b). All the primers used are listed in Supplemental Data Set S2. Final vectors were validated by sequencing and transformed into *A. tumefaciens* GV3101. As described by Shi et al. (2016b), *A. tumefaciens* cultures expressing GFP^N and GFP^C were mixed in equal volume and used to infiltrate leaves from 4- to 6-week-old *N. benthamiana*. All the *N. benthamiana* plants used for reciprocal BiFC assays were grown under the same environmental conditions, and leaves of similar age were used to test interactions between different pairs of proteins. Infiltrated leaves were examined with a confocal microscope as described previously (Shi et al., 2016b).

Accession Numbers

Sequence data of related genes/proteins can be found in the GenBank/EMBL databases under the following accession numbers: ORRM1, At3g20930; ORRM6, At1g73530; RIP1/MORF8, At3g15000; RIP2/MORF2, At2g33420; RIP9/MORF9, At1g11430; OZ1, At5g17790; LPA66, At5g48910; RARE1, At5g13270; PsbS, At1g44575; and ACTIN2, At3g18780.

Supplemental Data

The following supplemental materials are available.

Supplemental Figure S1. Protein sequence alignment of ORRMs.

Supplemental Figure S2. Positive controls for transient expression of ORRM1, LPA66, and RARE1 in *N. benthamiana* leaves.

Supplemental Figure S3. Relative transcript levels of select PSII genes in wild-type and *orrm6* mutant plants.

Supplemental Table S1. Relative abundances of select PSII proteins in wild-type and *orrm6* mutant plants.

Supplemental Data Set S1. Extents of chloroplast and mitochondrial RNA editing in wild-type and *orrm6-2* mutant plants determined via STS-PCR-seq.

Supplemental Data Set S2. Primers used in this study.

ACKNOWLEDGMENTS

We thank James P. O'Donnell, Krishna Nath, Kaley A. Walker, and Kelsey L. Walker for technical assistance; Christopher D. Jackson for Western Michigan University (WMU) growth chamber management; Peter Westhoff and Karin Meierhoff for sharing Gateway expression vector pAUL1; Jian Yao for sharing Gateway expression vector pPH5ADEST-CFP; John Kapenga and Elise DeDoncker for access to the WMU High Performance Computational Science Laboratory; Robert R. Evesole and Torin C. Kulhanek for access to WMU Biological Imaging Center; and Todd J. Barkman, Pamela Hoppe, Blair Szymczyna, and Jian Yao for comments on experimental design.

Received October 20, 2016; accepted February 13, 2017; published February 17, 2017.

LITERATURE CITED

Ajjawi I, Coku A, Froehlich JE, Yang Y, Osteryoung KW, Benning C, Last RL (2011) A J-like protein influences fatty acid composition of chloroplast lipids in Arabidopsis. PLoS ONE **6:** e25368

Baker NR, Harbinson J, Kramer DM (2007) Determining the limitations and regulation of photosynthetic energy transduction in leaves. Plant Cell Environ **30:** 1107–1125

Barkan A, Small I (2014) Pentatricopeptide repeat proteins in plants. Annu Rev Plant Biol **65:** 415–442

Bentolila S, Heller WP, Sun T, Babina AM, Friso G, van Wijk KJ, Hanson MR (2012) RIP1, a member of an Arabidopsis protein family, interacts with the protein RARE1 and broadly affects RNA editing. Proc Natl Acad Sci USA **109:** E1453–E1461

Bentolila S, Oh J, Hanson MR, Bukowski R (2013) Comprehensive high-resolution analysis of the role of an Arabidopsis gene family in RNA editing. PLoS Genet **9:** e1003584

Bock R (1998) Analysis of RNA editing in plastids. Methods **15:** 75–83

Bock R (2000) Sense from nonsense: how the genetic information of chloroplasts is altered by RNA editing. Biochimie **82:** 549–557

Bock R, Koop HU (1997) Extraplastidic site-specific factors mediate RNA editing in chloroplasts. EMBO J **16:** 3282–3288

Bock R, Kössel H, Maliga P (1994) Introduction of a heterologous editing site into the tobacco plastid genome: the lack of RNA editing leads to a mutant phenotype. EMBO J **13:** 4623–4628

Bondarava N, De Pascalis L, Al-Babili S, Goussias C, Golecki JR, Beyer P, Bock R, Krieger-Liszkay A (2003) Evidence that cytochrome b559 mediates the oxidation of reduced plastoquinone in the dark. J Biol Chem **278:** 13554–13560

Bonen L (2011) RNA splicing in plant mitochondria. *In* F Kempken, ed, Plant Mitochondria. Springer, New York, pp 131–155

Börner T, Zhelyazkova P, Legen J, Schmitz-Linneweber C (2014) Chloroplast gene expression: RNA synthesis and processing. *In* SM Theg, FA Wollman, eds, Plastid Biology. Springer, New York, pp 3–47

Cai W, Ji D, Peng L, Guo J, Ma J, Zou M, Lu C, Zhang L (2009) LPA66 is required for editing psbF chloroplast transcripts in Arabidopsis. Plant Physiol **150:** 1260–1271

Chateigner-Boutin AL, Small I (2007) A rapid high-throughput method for the detection and quantification of RNA editing based on high-resolution melting of amplicons. Nucleic Acids Res **35:** e114

Chateigner-Boutin AL, Small I (2010) Plant RNA editing. RNA Biol **7:** 213–219

Chateigner-Boutin AL, Small I (2011) Organellar RNA editing. Wiley Interdiscip Rev RNA **2:** 493–506

Chaudhuri S, Maliga P (1996) Sequences directing C to U editing of the plastid psbL mRNA are located within a 22 nucleotide segment spanning the editing site. EMBO J **15:** 5958–5964

Clark TJ, Lu Y (2015) Analysis of loss-of-function mutants in aspartate kinase and homoserine dehydrogenase genes points to complexity in the regulation of aspartate-derived amino acid contents. Plant Physiol **168:** 1512–1526

Clough SJ, Bent AF (1998) Floral dip: a simplified method for *Agrobacterium*-mediated transformation of *Arabidopsis thaliana*. Plant J **16:** 735–743

Colas des Francs-Small C, Small I (2014) Surrogate mutants for studying mitochondrially encoded functions. Biochimie **100:** 234–242

Dalby SJ, Bonen L (2013) Impact of low temperature on splicing of atypical group II introns in wheat mitochondria. Mitochondrion **13:** 647–655

Fang SC, Fernandez DE (2002) Effect of regulated overexpression of the MADS domain factor AGL15 on flower senescence and fruit maturation. Plant Physiol **130:** 78–89

Fujii S, Small I (2011) The evolution of RNA editing and pentatricopeptide repeat genes. New Phytol **191:** 37–47

Germain A, Hotto AM, Barkan A, Stern DB (2013) RNA processing and decay in plastids. Wiley Interdiscip Rev RNA **4:** 295–316

Hajdukiewicz P, Svab Z, Maliga P (1994) The small, versatile pPZP family of *Agrobacterium* binary vectors for plant transformation. Plant Mol Biol **25:** 989–994

Härtel B, Zehrmann A, Verbitskiy D, van der Merwe JA, Brennicke A, Takenaka M (2013) MEF10 is required for RNA editing at nad2-842 in mitochondria of Arabidopsis thaliana and interacts with MORF8. Plant Mol Biol **81:** 337–346

Hayes ML, Hanson MR (2007) Identification of a sequence motif critical for editing of a tobacco chloroplast transcript. RNA **13:** 281–288

Karamoko M, Cline S, Redding K, Ruiz N, Hamel PP (2011) Lumen Thiol Oxidoreductase1, a disulfide bond-forming catalyst, is required for the assembly of photosystem II in *Arabidopsis*. Plant Cell **23:** 4462–4475

Kiss AZ, Ruban AV, Horton P (2008) The PsbS protein controls the organization of the photosystem II antenna in higher plant thylakoid membranes. J Biol Chem **283:** 3972–3978

Levey T, Westhoff P, Meierhoff K (2014) Expression of a nuclear-encoded *psbH* gene complements the plastidic RNA processing defect in the PSII mutant hcf107 in *Arabidopsis thaliana*. Plant J **80:** 292–304

Li-Pook-Than J, Carrillo C, Niknejad N, Calixte S, Crosthwait J, Bonen L (2007) Relationship between RNA splicing and exon editing near intron junctions in wheat mitochondria. Physiol Plant **129:** 23–33

Lorković ZJ, Barta A (2002) Genome analysis: RNA recognition motif (RRM) and K homology (KH) domain RNA-binding proteins from the flowering plant Arabidopsis thaliana. Nucleic Acids Res **30:** 623–635

Lu Y (2011) The occurrence of a thylakoid-localized small zinc finger protein in land plants. Plant Signal Behav **6:** 1881–1885

Lu Y (2016) Identification and roles of photosystem II assembly, stability, and repair factors in Arabidopsis. Front Plant Sci **7:** 168

Lu Y, Hall DA, Last RL (2011a) A small zinc finger thylakoid protein plays a role in maintenance of photosystem II in *Arabidopsis thaliana*. Plant Cell **23:** 1861–1875

Lu Y, Savage LJ, Ajjawi I, Imre KM, Yoder DW, Benning C, Dellapenna D, Ohlrogge JB, Osteryoung KW, Weber APM, et al (2008) New connections across pathways and cellular processes: industrialized mutant screening reveals novel associations between diverse phenotypes in Arabidopsis. Plant Physiol **146:** 1482–1500

Lu Y, Savage LJ, Larson MD, Wilkerson CG, Last RL (2011b) Chloroplast 2010: a database for large-scale phenotypic screening of Arabidopsis mutants. Plant Physiol **155:** 1589–1600

Lu Y, Steichen JM, Yao J, Sharkey TD (2006) The role of cytosolic α-glucan phosphorylase in maltose metabolism and the comparison of amylomaltase in Arabidopsis and *Escherichia coli*. Plant Physiol **142:** 878–889

Lutz KA, Maliga P (2001) Lack of conservation of editing sites in mRNAs that encode subunits of the NAD(P)H dehydrogenase complex in plastids and mitochondria of *Arabidopsis thaliana*. Curr Genet **40:** 214–219

Müller P, Li XP, Niyogi KK (2001) Non-photochemical quenching: a response to excess light energy. Plant Physiol **125:** 1558–1566

Nath K, O'Donnell JP, Lu Y (2017) Chloroplastic iron-sulfur scaffold protein NFU3 is essential to overall plant fitness. Plant Signal Behav (in press) 10.1080/15592324.2017.1282023

Nath K, Wessendorf RL, Lu Y (2016) A nitrogen-fixing subunit essential for accumulating 4Fe-4S-containing photosystem I core proteins. Plant Physiol **172:** 2459–2470

Ohashi-Ito K, Bergmann DC (2006) *Arabidopsis* FAMA controls the final proliferation/differentiation switch during stomatal development. Plant Cell **18:** 2493–2505

O'Toole N, Hattori M, Andres C, Iida K, Lurin C, Schmitz-Linneweber C, Sugita M, Small I (2008) On the expansion of the pentatricopeptide repeat gene family in plants. Mol Biol Evol **25:** 1120–1128

Robbins JC, Heller WP, Hanson MR (2009) A comparative genomics approach identifies a PPR-DYW protein that is essential for C-to-U editing of the Arabidopsis chloroplast accD transcript. RNA **15:** 1142–1153

Roberson LM, Rosenthal JJ (2006) An accurate fluorescent assay for quantifying the extent of RNA editing. RNA **12:** 1907–1912

Ruwe H, Castandet B, Schmitz-Linneweber C, Stern DB (2013) Arabidopsis chloroplast quantitative editotype. FEBS Lett **587:** 1429–1433

Ruwe H, Kupsch C, Teubner M, Schmitz-Linneweber C (2011) The RNA-recognition motif in chloroplasts. J Plant Physiol **168:** 1361–1371

Sakamoto W, Miyagishima S, Jarvis P (2008) Chloroplast biogenesis: control of plastid development, protein import, division and inheritance. The Arabidopsis Book **6:** e0110,doi/0110.1199/tab.0110

Schallenberg-Rüdinger M, Kindgren P, Zehrmann A, Small I, Knoop V (2013) A DYW-protein knockout in Physcomitrella affects two closely spaced mitochondrial editing sites and causes a severe developmental phenotype. Plant J **76:** 420–432

Schmitz-Linneweber C, Barkan A (2007) RNA splicing and RNA editing in chloroplasts. *In* R Bock, ed, Cell and Molecular Biology of Plastids. Springer, Berlin, pp 213–248

Schmitz-Linneweber C, Small I (2008) Pentatricopeptide repeat proteins: a socket set for organelle gene expression. Trends Plant Sci **13:** 663–670

Sessions A, Burke E, Presting G, Aux G, McElver J, Patton D, Dietrich B, Ho P, Bacwaden J, Ko C, et al (2002) A high-throughput *Arabidopsis* reverse genetics system. Plant Cell **14:** 2985–2994

Shi X, Bentolila S, Hanson MR (2016a) Organelle RNA recognition motif-containing (ORRM) proteins are plastid and mitochondrial editing factors in Arabidopsis. Plant Signal Behav **11:** e1167299

Shi X, Germain A, Hanson MR, Bentolila S (2016b) RNA recognition motif-containing protein ORRM4 broadly affects mitochondrial RNA editing and impacts plant development and flowering. Plant Physiol **170:** 294–309

Shi X, Hanson MR, Bentolila S (2015) Two RNA recognition motif-containing proteins are plant mitochondrial editing factors. Nucleic Acids Res **43:** 3814–3825

Shikanai T (2015) RNA editing in plants: machinery and flexibility of site recognition. Biochim Biophys Acta **1847:** 779–785

Sparkes IA, Runions J, Kearns A, Hawes C (2006) Rapid, transient expression of fluorescent fusion proteins in tobacco plants and generation of stably transformed plants. Nat Protoc **1:** 2019–2025

Sun T, Bentolila S, Hanson MR (2016) The unexpected diversity of plant organelle RNA editosomes. Trends Plant Sci **21:** 962–973

Sun T, Germain A, Giloteaux L, Hammani K, Barkan A, Hanson MR, Bentolila S (2013) An RNA recognition motif-containing protein is required for plastid RNA editing in Arabidopsis and maize. Proc Natl Acad Sci USA **110:** E1169–E1178

Sun T, Shi X, Friso G, Van Wijk K, Bentolila S, Hanson MR (2015) A zinc finger motif-containing protein is essential for chloroplast RNA editing. PLoS Genet **11:** e1005028

Takenaka M, Zehrmann A, Verbitskiy D, Härtel B, Brennicke A (2013) RNA editing in plants and its evolution. Annu Rev Genet **47:** 335–352

Takenaka M, Zehrmann A, Verbitskiy D, Kugelmann M, Härtel B, Brennicke A (2012) Multiple organellar RNA editing factor (MORF) family proteins are required for RNA editing in mitochondria and plastids of plants. Proc Natl Acad Sci USA **109:** 5104–5109

Tillich M, Funk HT, Schmitz-Linneweber C, Poltnigg P, Sabater B, Martin M, Maier RM (2005) Editing of plastid RNA in *Arabidopsis thaliana* ecotypes. Plant J **43:** 708–715

Wang S, Bai G, Wang S, Yang L, Yang F, Wang Y, Zhu JK, Hua J (2016) Chloroplast RNA-binding protein RBD1 promotes chilling tolerance through 23S rRNA processing in Arabidopsis. PLoS Genet **12:** e1006027

Wang W, Zhang W, Wu Y, Maliga P, Messing J (2015) RNA editing in chloroplasts of *Spirodela polyrhiza*, an aquatic monocotyledonous species. PLoS ONE **10:** e0140285

Wellburn AR (1994) The spectral determination of chlorophyll *a* and chlorophyll *b*, as well as total carotenoids, using various solvents with spectrophotometers of different resolution. J Plant Physiol **144:** 307–313

Withers J, Yao J, Mecey C, Howe GA, Melotto M, He SY (2012) Transcription factor-dependent nuclear localization of a transcriptional repressor in jasmonate hormone signaling. Proc Natl Acad Sci USA **109:** 20148–20153

Woody ST, Austin-Phillips S, Amasino RM, Krysan PJ (2007) The WiscDsLox T-DNA collection: an Arabidopsis community resource generated by using an improved high-throughput T-DNA sequencing pipeline. J Plant Res **120:** 157–165

Yang Y, Sage TL, Liu Y, Ahmad TR, Marshall WF, Shiu SH, Froehlich JE, Imre KM, Osteryoung KW (2011) CLUMPED CHLOROPLASTS 1 is required for plastid separation in Arabidopsis. Proc Natl Acad Sci USA **108:** 18530–18535

Yohn CB, Cohen A, Danon A, Mayfield SP (1998) A poly(A) binding protein functions in the chloroplast as a message-specific translation factor. Proc Natl Acad Sci USA **95:** 2238–2243

Zoschke R, Kupsch C, Schmitz-Linneweber C (2011) RNA-binding proteins required for chloroplast RNA processing. *In* F Kempken, ed, Plant Mitochondria. Springer, New York, pp 177–203